DE GRUYTER OPEN

Int. J. of Applied Mechanics and Engineering, 2016, vol.21, No.2, pp.359-376
DOI: 10.1515/ijame-2016-0022

THREE DIMENSIONAL FLOW AND MASS TRANSFER ANALYSIS OF A SECOND GRADE FLUID IN A POROUS CHANNEL WITH A LOWER STRETCHING WALL

N.A. KHAN* and F. NAZ
Department of Mathematics, University of Karachi
Karachi 75270, PAKISTAN
E-mail: njbalam@yahoo.com

This investigation analyses a three dimensional flow and mass transfer of a second grade fluid over a porous stretching wall in the presence of suction or injection. The equations governing the flow are attained in terms of partial differential equations. A similarity transformation has been utilized for the transformation of partial differential equations into the ordinary differential equations. The solutions of the nonlinear systems are given by the homotopy analysis method (HAM). A comparative study with the previous results of a viscous fluid has been made. The convergence of the series solution has also been considered explicitly. The influence of admissible parameters on the flows is delineated through graphs and appropriate results are presented. In addition, it is found that instantaneous suction and injection reduce viscous drag on the stretching sheet. It is also shown that suction or injection of a fluid through the surface is an example of mass transfer and it can change the flow field.

Key words: second grade fluid; stretching wall; suction; injection

1. Introduction

Non-Newtonian fluids have attracted the attention of researchers during the past few decades because of their wide-ranging industrial and technological applications. It is well known that it is insufficient to employ Newton's law of viscosity for considering the behavior of non-Newtonian fluid dynamics. A single constitutive relationship between shear stress and rate of strain cannot be used to examine these types of fluids. There are various constitutive equations that are available to analyze the diverse characteristics of non-Newtonian fluids. Many non- Newtonian fluids of differential types that are used to explain the non-Newtonian behavior have achieved much importance because of well established applications in different fields. There is a large class of applications of non-Newtonian fluids that are used in various fields of science, engineering and technology especially in material processing, chemical industry and bio-engineering. Furthermore, applications in non-Newtonian fluids include petroleum drilling, paper production, glass blowing, and plastic sheet formation. There is also a significant interest of non-Newtonian fluid flow in oil reservoir engineering and furthermore the non-Newtonian fluids, such as mercury amalgams, liquid metals, biological fluids, plastic extrusions, paper coating and lubrication oils, have applications in many fields. The flow characteristics of non-Newtonian fluids are relatively different from those of Newtonian fluids. Due to the complexity of flow behavior, non-Newtonian fluids can be recognized on the basis of their behavior in shear.

The constitutive equation of a second grade fluid consist a linear relation between the stress and the first Rivlin-Ericksen tensor, the square of the first Rivlin-Ericksen tensor and the second Rivlin-Ericksen tensor. This equation contains three coefficients and these coefficients have some restrictions. Dunn and Fosdick [1] as well as Dunn and Rajagopal [2] discussed the restrictions of the coefficients. Ali *et al*. [3] studied the problem related to the steady plane flow of a second grade fluid and employed Martin's method.

---

* To whom correspondence should be addressed

Khan *et al*. [4] considered the flow of a second grade fluid between two longitudinally oscillating cylinders and provided exact analytic solutions for this flow. Hayat *et al*. [5] studied an unsteady Couette flow of a second grade fluid in a layer of a porous medium. Abdallah [6] obtained an analytical solution of heat and mass transfer over a permeable stretching plate affected by a chemical reaction, internal heating, the Dufour-Souret effect and Hall effect. Exact solutions of flow problems of a second grade fluid through two parallel porous walls were extensively discussed by Ariel [7]. The unsteady unidirectional flow of a second grade fluid between the parallel plates with different given volume flow rate conditions was examined by Chen *et al*. [8].

The study of flow over a stretching wall has gained much importance in recent years due to its various industrial uses, e.g., in polymer sheets, artificial fibers and manufacturing and rolling plastic films. Various researchers are engaged in examining the effects of non-Newtonian fluids by considering the flow over a stretching wall. Aksoy *et al*. [9] presented the boundary layer equations and stretching sheet solutions for a modified second grade fluid. Hayat and Sajid [10] found an analytical solution for an axisymmetric flow and heat transfer of a second grade fluid past a stretching sheet. Further existence results for classical solutions of the equations of a second-grade fluid were discussed by Galdi and Sequeira [11]. Cortell [12] studied the MHD flow and mass transfer of an electrically conducting fluid of second grade in a porous medium over a stretching sheet with chemically reactive species. Ellahi [13] observed the effects of an MHD flow and temperature dependent viscosity on the flow of a non-Newtonian nanofluid in a pipe. Hayat et al. [14] obtained a homotopy solution for an unsteady three-dimensional MHD flow and mass transfer in a porous space. Hayat *et al*. [15] considered a mixed convection boundary layer flow of a Maxwell fluid over a stretching surface. This boundary layer flow was studied with Soret and Dufour effects. Abel *et al*. [16] considered the heat transfer due to an MHD slip flow of a second-grade liquid over a stretching sheet through a porous medium with a non uniform heat source/sink. Zeeshan and Ellahi [17] considered the non-Newtonian MHD fluid flow in a porous space with slip boundary conditions. Ellahi *et al*. [18] presented the steady flow of a Couette fluid with the effects of heat transfer and nonlinear slip. The flow behavior of nanofluids over a permeable stretching wall with the effects of heat transfer was considered by Sheikholeslami *et al*. [19]. Mehmood and Ali [20] studied the across mass transfer phenomenon in a channel of a lower stretching wall. A thermal analysis of flow in a porous medium over a permeable stretching wall was proposed by Tamayol *et al*. [21]. Raftari and Vajravelu [22] used the homotopy analysis method to analyze an MHD viscoelastic fluid flow and heat transfer in a channel with a stretching wall.

Mehmood and Ali [23] made a heat transfer analysis of a three-dimensional flow in a channel of a lower stretching wall. A three-dimensional squeezing flow in a rotating channel of a lower stretching porous wall was discussed by Munawar *et al*. [24]. A three dimensional flow of a viscoelastic fluid by an exponentially stretching surface with mass transfer was examined by Alhuthali *et al*. [25]. Nadeem *et al*. [26] studied the MHD three-dimensional Casson fluid flow past a porous linearly stretching sheet. A study related to the heat and mass transfer in a Jeffrey fluid over a stretching sheet with heat source/sink was given by Qasim [27]. The associated heat transfer in a second grade fluid through a porous medium from a permeable stretching sheet with non-uniform heat source/sink problem was examined recently by Abel *et al*. [28]. Hayat *et al*. [29] presented the three-dimensional flow of a Jeffery fluid over a linearly stretching sheet.

The aim of the present study is to examine a three-dimensional flow for the second grade fluid over a stretching wall and this problem also involves the mass transfer phenomenon in the presence of suction and injection. The resulting nonlinear partial differential equations are reduced into nonlinear ordinary differential equations by similarity transformation. The homotopy analysis method (HAM) is employed to compute series solutions of the flow equations. We also present effects of pertinent parameters in the series solutions by plotting graphs.

2. Physical problem and mathematical formulations

Let us assume an incompressible second grade fluid flow between two infinite parallel plane plates situated at $z = 0$ and $z = h$. Suction/ injection can be obtained by assuming that both the plates are porous.

The lower plate is being stretched in two lateral directions with different rates and the z-axis is taken perpendicular to the plates as schematically shown in Fig.1. The governing system of equations is given as

$$\boldsymbol{T} = -p\boldsymbol{I} + \mu\, \boldsymbol{A_1} + \alpha_1\, \boldsymbol{A_2} + \alpha_2\, \boldsymbol{A_1^2} \tag{2.1}$$

where p is the pressure, $\boldsymbol{I}$ is the unit vector, α_1 and α_2 are normal stress moduli, $\boldsymbol{A_1}$ and $\boldsymbol{A_2}$ are the kinematical tensors and these tensors can be written as

$$\left(\boldsymbol{A_1}, \boldsymbol{A_2}\right) = \left(M + M^{\tau}, \frac{D}{Dt}\boldsymbol{A_1} + M.\boldsymbol{A_1} + \boldsymbol{A_1}.M^{\tau} \right), M = \nabla V. \tag{2.2}$$

The laws of conservation of mass and momentum for the present flow problem are given by

$$\nabla . V = 0, \tag{2.3}$$

$$\left(V.\nabla\right) u = -\frac{1}{\rho}\frac{\partial p}{\partial x} + \frac{1}{\rho}\left(\frac{\partial T_{11}}{\partial x} + \frac{\partial T_{12}}{\partial y} + \frac{\partial T_{13}}{\partial z} \right), \tag{2.4}$$

$$\left(V.\nabla\right) v = -\frac{1}{\rho}\frac{\partial p}{\partial y} + \frac{1}{\rho}\left(\frac{\partial T_{21}}{\partial x} + \frac{\partial T_{22}}{\partial y} + \frac{\partial T_{23}}{\partial z} \right), \tag{2.5}$$

$$\left(V.\nabla\right) w = -\frac{1}{\rho}\frac{\partial p}{\partial z} + \frac{1}{\rho}\left(\frac{\partial T_{31}}{\partial x} + \frac{\partial T_{32}}{\partial y} + \frac{\partial T_{33}}{\partial z} \right) \tag{2.6}$$

where

$$\begin{aligned}\boldsymbol{T_{11}} = {} & 2\mu\frac{\partial u}{\partial x} + \alpha_1\left(2u\frac{\partial^2 u}{\partial x^2} + 2v\frac{\partial^2 u}{\partial x \partial y} + 2w\frac{\partial^2 u}{\partial x \partial z} + 4\left(\frac{\partial u}{\partial x}\right)^2 + 2\frac{\partial v}{\partial x}\left(\frac{\partial u}{\partial y} + \frac{\partial v}{\partial x}\right) + \right. \\ & \left. +2\frac{\partial w}{\partial x}\left(\frac{\partial u}{\partial z} + \frac{\partial w}{\partial x}\right)\right) + \alpha_2\left(4\left(\frac{\partial u}{\partial x}\right)^2 + \left(\frac{\partial u}{\partial y} + \frac{\partial v}{\partial x}\right)^2 + \left(\frac{\partial w}{\partial x} + \frac{\partial u}{\partial z}\right)^2 \right),\end{aligned} \tag{2.7}$$

$$\begin{aligned}\boldsymbol{T_{12}} = \boldsymbol{T_{21}} = {} & \mu\left(\frac{\partial u}{\partial y} + \frac{\partial v}{\partial x}\right) + \alpha_1\left(u\frac{\partial^2 u}{\partial y \partial x} + u\frac{\partial^2 v}{\partial x^2} + v\left(\frac{\partial^2 u}{\partial y^2} + \frac{\partial^2 v}{\partial x \partial y}\right) + w\left(\frac{\partial^2 u}{\partial y \partial z} + \frac{\partial^2 v}{\partial x \partial z}\right) + \right. \\ & \left. +3\frac{\partial u}{\partial x}\frac{\partial u}{\partial y} + \frac{\partial v}{\partial y}\frac{\partial u}{\partial y} + \frac{\partial u}{\partial x}\frac{\partial v}{\partial x} + 3\frac{\partial v}{\partial x}\frac{\partial v}{\partial y} + v\frac{\partial v}{\partial y}\left(\frac{\partial u}{\partial z} + \frac{\partial w}{\partial x}\right) + \frac{\partial w}{\partial x}\left(\frac{\partial w}{\partial y} + \frac{\partial v}{\partial z}\right)\right) + \\ & +\alpha_2\left(2\frac{\partial u}{\partial x}\left(\frac{\partial u}{\partial y} + \frac{\partial v}{\partial x}\right) + 2\frac{\partial v}{\partial y}\left(\frac{\partial u}{\partial y} + \frac{\partial v}{\partial x}\right) + \left(\frac{\partial u}{\partial z} + \frac{\partial w}{\partial x}\right)\left(\frac{\partial w}{\partial y} + \frac{\partial v}{\partial z}\right)\right),\end{aligned} \tag{2.8}$$

$$\begin{aligned}
\boldsymbol{T_{13}}=\boldsymbol{T_{31}}=\mu\left(\frac{\partial u}{\partial z}+\frac{\partial w}{\partial x}\right)+\alpha_1\Bigg(&u\frac{\partial^2 u}{\partial z\partial x}+u\frac{\partial^2 w}{\partial x^2}+v\frac{\partial^2 u}{\partial z\partial y}+v\frac{\partial^2 w}{\partial x\partial y}+w\frac{\partial^2 u}{\partial z^2}+w\frac{\partial^2 w}{\partial x\partial z}+\\
&+3\frac{\partial u}{\partial x}\frac{\partial u}{\partial z}+2\frac{\partial v}{\partial z}\frac{\partial v}{\partial x}+\frac{\partial v}{\partial z}\frac{\partial u}{\partial y}+\frac{\partial w}{\partial z}\frac{\partial u}{\partial z}+\frac{\partial u}{\partial x}\frac{\partial w}{\partial x}+\frac{\partial v}{\partial x}\frac{\partial w}{\partial y}+3\frac{\partial w}{\partial x}\frac{\partial w}{\partial z}\Bigg)+\\
&+\alpha_2\left(2\frac{\partial u}{\partial x}\left(\frac{\partial u}{\partial z}+\frac{\partial w}{\partial x}\right)+\left(\frac{\partial u}{\partial y}+\frac{\partial v}{\partial x}\right)\left(\frac{\partial v}{\partial z}+\frac{\partial w}{\partial y}\right)+2\frac{\partial w}{\partial z}\left(\frac{\partial u}{\partial z}+\frac{\partial w}{\partial x}\right)\right),
\end{aligned}\tag{2.9}$$

$$\begin{aligned}
\boldsymbol{T_{22}}=2\mu\left(\frac{\partial v}{\partial y}\right)+\alpha_1\Bigg(&2u\frac{\partial^2 v}{\partial y\partial x}+2v\frac{\partial^2 v}{\partial y^2}+2w\frac{\partial^2 v}{\partial y\partial z}+4\left(\frac{\partial v}{\partial y}\right)^2+2\frac{\partial u}{\partial y}\left(\frac{\partial v}{\partial x}+\frac{\partial u}{\partial y}\right)+\\
&+2\frac{\partial w}{\partial y}\left(\frac{\partial v}{\partial z}+\frac{\partial w}{\partial y}\right)\Bigg)+\alpha_2\left(4\left(\frac{\partial v}{\partial y}\right)^2+\left(\frac{\partial u}{\partial y}+\frac{\partial v}{\partial x}\right)^2+\left(\frac{\partial v}{\partial z}+\frac{\partial w}{\partial y}\right)^2\right),
\end{aligned}\tag{2.10}$$

$$\begin{aligned}
\boldsymbol{T_{23}}=\boldsymbol{T_{32}}=\mu\left(\frac{\partial v}{\partial z}+\frac{\partial w}{\partial y}\right)+\alpha_1\Bigg(&u\frac{\partial^2 v}{\partial z\partial x}+u\frac{\partial^2 w}{\partial y\partial x}+v\frac{\partial^2 v}{\partial z\partial y}+v\frac{\partial^2 w}{\partial y^2}+w\frac{\partial^2 v}{\partial z^2}+w\frac{\partial^2 w}{\partial y\partial z}+\\
&+\frac{\partial u}{\partial z}\frac{\partial v}{\partial x}+2\frac{\partial u}{\partial z}\frac{\partial u}{\partial y}+3\frac{\partial v}{\partial y}\frac{\partial v}{\partial z}+\frac{\partial w}{\partial z}\frac{\partial v}{\partial z}+\frac{\partial u}{\partial y}\frac{\partial w}{\partial x}+\frac{\partial v}{\partial y}\frac{\partial w}{\partial y}+3\frac{\partial w}{\partial y}\frac{\partial w}{\partial z}\Bigg)+\\
&+\alpha_2\left(2\frac{\partial v}{\partial y}\left(\frac{\partial v}{\partial z}+\frac{\partial w}{\partial y}\right)+2\frac{\partial w}{\partial z}\left(\frac{\partial v}{\partial z}+\frac{\partial w}{\partial y}\right)+\left(\frac{\partial v}{\partial x}+\frac{\partial u}{\partial y}\right)\left(\frac{\partial u}{\partial z}+\frac{\partial w}{\partial x}\right)\right),
\end{aligned}\tag{2.11}$$

$$\begin{aligned}
\boldsymbol{T_{33}}=2\mu\left(\frac{\partial w}{\partial z}\right)+\alpha_1\Bigg(&2u\frac{\partial^2 w}{\partial z\partial x}+2v\frac{\partial^2 w}{\partial z\partial y}+2w\frac{\partial^2 w}{\partial z^2}+4\left(\frac{\partial w}{\partial z}\right)^2+\\
&+2\frac{\partial u}{\partial z}\left(\frac{\partial w}{\partial x}+\frac{\partial u}{\partial z}\right)+2\frac{\partial v}{\partial z}\left(\frac{\partial w}{\partial y}+\frac{\partial v}{\partial z}\right)\Bigg)+\alpha_2\left(4\left(\frac{\partial w}{\partial z}\right)^2+\left(\frac{\partial w}{\partial x}+\frac{\partial u}{\partial z}\right)^2+\left(\frac{\partial v}{\partial z}+\frac{\partial w}{\partial y}\right)^2\right),
\end{aligned}\tag{2.12}$$

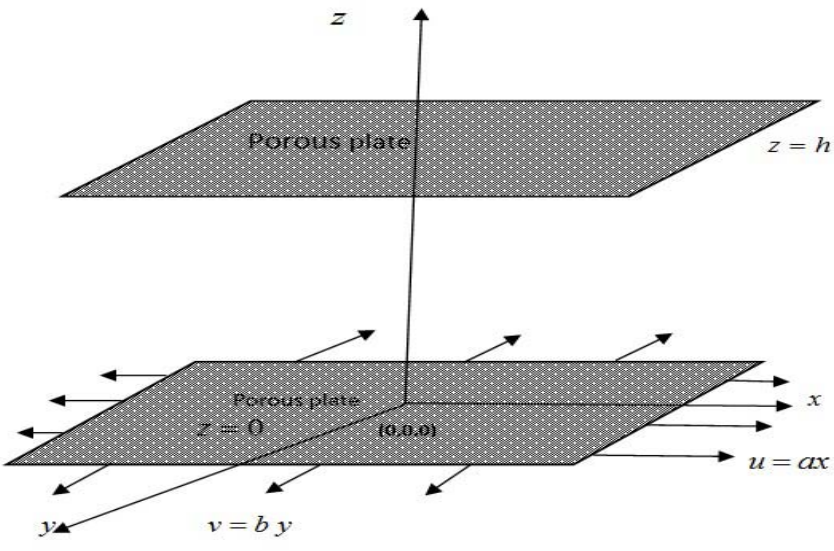

Fig.1. Schematic diagram and flow configuration of the problem

The boundary conditions applicable to the flow problem are

$$u = a\ x \qquad v = by \qquad w = -w_0^* \qquad \text{at} \qquad z = 0. \tag{2.13}$$

$$u = 0 \qquad v = 0 \qquad w = -w_1^* \qquad \text{at} \qquad z = h. \tag{2.14}$$

Here a and b represent velocity gradients, h is width of the channel and w_0^*, w_1^* are suction/ injection velocities at the lower and upper walls. The similarity transformation is presented as

$$(u,v,w,\eta) = \left(a\ x f'\ (\eta), a\ y\ g'(\eta), -a\ h\big(f(\eta)+g(\eta)\big), \frac{1}{h}z \right). \tag{2.15}$$

By using the above similarity transformations in Eqs (2.3)-(2.6), the equation of continuity is satisfied whereas the governing partial differential equations are reduced to the following form

$$\begin{aligned} &f'''' + \mathrm{Re}\left(g' f'' - f' f'' + f f''' + g f'''\right) + \\ &+\mathrm{We}\begin{pmatrix} 16 f'' f''' - 3g'' f''' - f'' g'' + f' f'''' - 3g' f'''' - f f''''' - g f''''' + \\ +\lambda\left(8 f'' f''' - 3\ g'' f''' - f'' g''' - 2g' f''''\right) \end{pmatrix} = 0, \end{aligned} \tag{2.16}$$

$$\begin{aligned} &g'''' + \mathrm{Re}\left(f' g'' - g' g'' + f g''' + gg'''\right) + \\ &+\mathrm{We}\begin{pmatrix} 16\ g'' g''' - 3 f'\ g'''' + g'\ g'''' - f\ g''''' - g\ g''''' - g'' f''' - 3 f'' g''' + \\ +\lambda\left(8\ g'' g''' - 2 f'\ g'''' - g'' f''' - 3 f'' g''\right) \end{pmatrix} = 0, \end{aligned} \tag{2.17}$$

and the boundary conditions are transformed to

$$\begin{aligned} &f'(0) = 1, \qquad g'(0) = \beta, \qquad f(0) + g(0) = w_0, \\ &f'(1) = 0, \qquad g'(1) = 0, \qquad f(1) + g(1) = w_1 \end{aligned} \tag{2.18}$$

where $\lambda = \dfrac{\alpha_2}{\alpha_1}$ is the ratio of normal stress moduli, $\mathrm{We} = \dfrac{a\alpha_1}{\mu}$ is the Weissenberg number, $\mathrm{Re} = \dfrac{ah^2}{\nu}$ is the Reynolds number, $w_0 = \dfrac{w_0^*}{ah}$, and $w_1 = \dfrac{w_1^*}{ah}$ are the suction/injection velocities at lower and upper walls, $\beta = \dfrac{b}{a}(a \neq 0)$ is the ratio of the velocity gradients and primes denote the differentiation with respect to η. The pressure p can be obtained by

$$p = p_0 - \frac{1}{2}\rho\, a^2\left(x^2 + y^2\right) - \frac{w^2}{2} + 2\mu w_z + 5\alpha_1 w_z^2 + 4\ \alpha_2 w_z^2 \tag{2.19}$$

where “ p_0 ” is the pressure at origin and “ ρ ”is the fluid density. At the stretching plate, the skin friction coefficients in the x-and y-directions have been calculated as,

$$\tau_{xz}=\frac{1}{\rho(ax)^2}\left(\begin{array}{l}\mu\left(\frac{\partial u}{\partial z}+\frac{\partial w}{\partial x}\right)+\alpha_1\left(\begin{array}{l}u\frac{\partial^2 u}{\partial z\partial x}+u\frac{\partial^2 w}{\partial x^2}+v\frac{\partial^2 u}{\partial z\partial y}+v\frac{\partial^2 w}{\partial x\partial y}+w\frac{\partial^2 u}{\partial z^2}+w\frac{\partial^2 w}{\partial x\partial z}+2\frac{\partial u}{\partial x}\frac{\partial u}{\partial z}+\frac{\partial v}{\partial z}\frac{\partial u}{\partial y}+\\+\frac{\partial v}{\partial x}\frac{\partial v}{\partial z}+\frac{\partial u}{\partial z}\frac{\partial w}{\partial z}+\frac{\partial w}{\partial x}\frac{\partial w}{\partial z}+\frac{\partial u}{\partial x}\frac{\partial u}{\partial z}+\frac{\partial w}{\partial x}\frac{\partial u}{\partial x}+\frac{\partial v}{\partial x}\frac{\partial v}{\partial z}+\frac{\partial w}{\partial y}\frac{\partial v}{\partial x}+2\frac{\partial w}{\partial x}\frac{\partial w}{\partial z}\end{array}\right)+\\+\alpha_2\left(2\frac{\partial u}{\partial x}\frac{\partial u}{\partial z}+2\frac{\partial u}{\partial x}\frac{\partial w}{\partial x}+\frac{\partial u}{\partial y}\frac{\partial v}{\partial z}+\frac{\partial u}{\partial y}\frac{\partial w}{\partial y}+\frac{\partial v}{\partial x}\frac{\partial v}{\partial z}+\frac{\partial v}{\partial x}\frac{\partial w}{\partial y}+2\frac{\partial u}{\partial z}\frac{\partial w}{\partial z}+2\frac{\partial w}{\partial x}\frac{\partial w}{\partial z}\right)\end{array}\right)\Bigg|_{z=0}=$$

$$=\mathrm{Re}^{-\frac{1}{2}}\mathrm{Re}_x^{-\frac{1}{2}}\left[f''(0)+\mathrm{We}\left(f''(0)\left(3f'(0)-g'(0)-2\lambda g'(0)\right)-f'''(0)\left(f(0)+g(0)\right)\right)\right], \tag{2.20}$$

$$\tau_{yz}=\frac{1}{\rho(a\,y)^2}\left(\begin{array}{l}\mu\left(\frac{\partial w}{\partial y}+\frac{\partial v}{\partial z}\right)+\alpha_1\left(\begin{array}{l}u\frac{\partial^2 w}{\partial y\partial x}+u\frac{\partial^2 v}{\partial z\partial x}+v\frac{\partial^2 w}{\partial y^2}+v\frac{\partial^2 v}{\partial z\partial y}+w\frac{\partial^2 w}{\partial y\partial z}+w\frac{\partial^2 v}{\partial z^2}+\frac{\partial u}{\partial y}\frac{\partial w}{\partial x}+\frac{\partial u}{\partial y}\frac{\partial u}{\partial z}\\+\frac{\partial v}{\partial y}\frac{\partial w}{\partial y}+\frac{\partial v}{\partial y}\frac{\partial v}{\partial z}+2\frac{\partial w}{\partial y}\frac{\partial w}{\partial z}+\frac{\partial u}{\partial y}\frac{\partial u}{\partial z}+\frac{\partial v}{\partial x}\frac{\partial u}{\partial z}+2\frac{\partial v}{\partial y}\frac{\partial v}{\partial z}+\frac{\partial w}{\partial y}\frac{\partial w}{\partial z}+\frac{\partial v}{\partial z}\frac{\partial w}{\partial z}\end{array}\right)\\+\alpha_2\left(\frac{\partial w}{\partial x}\frac{\partial u}{\partial y}+\frac{\partial w}{\partial x}\frac{\partial v}{\partial x}+\frac{\partial u}{\partial z}\frac{\partial u}{\partial y}+\frac{\partial u}{\partial z}\frac{\partial v}{\partial x}+2\frac{\partial v}{\partial y}\frac{\partial w}{\partial y}+2\frac{\partial v}{\partial y}\frac{\partial v}{\partial z}+2\frac{\partial w}{\partial z}\frac{\partial w}{\partial y}+2\frac{\partial v}{\partial z}\frac{\partial w}{\partial z}\right)\end{array}\right)\Bigg|_{z=0}=$$

$$=\mathrm{Re}^{-\frac{1}{2}}\mathrm{Re}_y^{-\frac{1}{2}}\left[g''(0)+We\left(g''(0)\left(3g'(0)-f'(0)-2\lambda f'(0)\right)-g'''(0)\left(f(0)+g(0)\right)\right)\right] \tag{2.21}$$

where $\mathrm{Re}_x=\frac{ax^2}{\upsilon}$ and $\mathrm{Re}_y=\frac{ay^2}{\upsilon}$ are local Reynolds numbers. Also, Eqs (2.16)-(2.17) represent the system of second grade fluid equations. However, if the value of We is set to zero in the system, it will reduce to the viscous fluid equations [20].

3. Solution of a second grade fluid in a channel of a lower stretching wall

Liao [30] suggested a new kind of an analytical method for solving nonlinear problems, explicitly known as the homotopy analysis method (HAM). This technique is mainly based on the homotopy from the concept of topology. HAM does not depend upon whether or not nonlinear equations under consideration hold small or large parameters, hence this method can solve more of powerfully nonlinear equations [31-32] as compared with perturbation techniques. Moreover, it gives us great freedom to choose auxiliary linear operators and initial guesses and gives a family of approximations which are converging in a large region. The auxiliary linear operator $\mathrm{L}=[f,g]$ is selected for Eqs (2.16)- (2.17)

$$\mathrm{L}=\frac{d^4}{d\eta^4}\,. \tag{3.1}$$

Also, the initial guesses for the approximations satisfying the initial conditions in Eq.(2.18)

$$f_0(\eta)=\frac{1}{2}w_0+\eta+\left(\frac{3}{2}w_1-2-\frac{3}{2}w_0\right)\eta^2+\left(1-w_1+w_0\right)\eta^3 \tag{3.2}$$

$$g_0(\eta)=\frac{1}{2}w_0+\beta\,\eta+\left(\frac{3}{2}w_1-2\beta-\frac{3}{2}w_0\right)\eta^2+\left(\beta-w_1+w_0\right)\eta^3, \tag{3.3}$$

satisfying the following properties

$$\mathrm{L}\left[c_1+c_2\eta+c_3\eta^2+c_4\eta^3\right]=0 \tag{3.4}$$

where c_1, c_2, c_3 and c_4 are arbitrary constants. The zeroth order deformation equations can be made as

$$(1-p)\mathrm{L}\left[\left(\tilde{F}(\eta;p),\tilde{G}(\eta;p)\right)-\left(f_0(\eta),g_0(\eta)\right)\right]-p\left[\hbar_f N_f\left(\tilde{F}(\eta;p),\tilde{G}(\eta;p)\right),\hbar_g N_g\left(\tilde{F}(\eta;p),\tilde{G}(\eta;p)\right)\right]=0 \tag{3.5}$$

where

$$\begin{aligned}N_f\left[\tilde{F}(\eta;p),\tilde{G}(\eta;p)\right]=&\frac{\partial^4\tilde{F}(\eta;p)}{\partial\eta^4}+\mathrm{Re}\left(\begin{array}{l}\dfrac{\partial\tilde{G}(\eta;p)}{\partial\eta}\dfrac{\partial^2\tilde{F}(\eta;p)}{\partial\eta^2}-\dfrac{\partial\tilde{F}(\eta;p)}{\partial\eta}\dfrac{\partial^2\tilde{F}(\eta;p)}{\partial\eta^2}+\tilde{F}(\eta;p)\dfrac{\partial^3\tilde{F}(\eta;p)}{\partial\eta^3}+\\+\tilde{G}(\eta;p)\dfrac{\partial^3\tilde{F}(\eta;p)}{\partial\eta^3}\end{array}\right)+\\&+\mathrm{We}\left(\begin{array}{l}16\,\dfrac{\partial^2\tilde{F}(\eta;p)}{\partial\eta^2}\dfrac{\partial^3\tilde{F}(\eta;p)}{\partial\eta^3}-3\,\dfrac{\partial^2\tilde{G}(\eta;p)}{\partial\eta^2}\dfrac{\partial^3\tilde{F}(\eta;p)}{\partial\eta^3}-\dfrac{\partial^2\tilde{F}(\eta;p)}{\partial\eta^2}\dfrac{\partial^3\tilde{G}(\eta;p)}{\partial\eta^3}+\dfrac{\partial\tilde{F}(\eta;p)}{\partial\eta}\dfrac{\partial^4\tilde{F}(\eta;p)}{\partial\eta^4}+\\-3\,\dfrac{\partial\tilde{G}(\eta;p)}{\partial\eta}\dfrac{\partial^4\tilde{F}(\eta;p)}{\partial\eta^4}-\tilde{F}(\eta;p)\dfrac{\partial^5\tilde{F}(\eta;p)}{\partial\eta^5}-\tilde{G}(\eta;p)\dfrac{\partial^5\tilde{F}(\eta;p)}{\partial\eta^5}+\\+\lambda\left(8\,\dfrac{\partial^2\tilde{F}(\eta;p)}{\partial\eta^2}\dfrac{\partial^3\tilde{F}(\eta;p)}{\partial\eta^3}-3\dfrac{\partial^2\tilde{G}(\eta;p)}{\partial\eta^2}\dfrac{\partial^3\tilde{F}(\eta;p)}{\partial\eta^3}-\dfrac{\partial^2\tilde{F}(\eta;p)}{\partial\eta^2}\dfrac{\partial^3\tilde{G}(\eta;p)}{\partial\eta^3}-2\dfrac{\partial\tilde{G}(\eta;p)}{\partial\eta}\dfrac{\partial^4\tilde{F}(\eta;p)}{\partial\eta^4}\right)\end{array}\right).\end{aligned} \tag{3.6}$$

$$\begin{aligned}N_g\left[\tilde{F}(\eta;p),\tilde{G}(\eta;p)\right]=&\frac{\partial^4\tilde{G}(\eta;p)}{\partial\eta^4}+\mathrm{Re}\left(\begin{array}{l}\dfrac{\partial\tilde{F}(\eta;p)}{\partial\eta}\dfrac{\partial^2\tilde{G}(\eta;p)}{\partial\eta^2}-\dfrac{\partial\tilde{G}(\eta;p)}{\partial\eta}\dfrac{\partial^2\tilde{G}(\eta;p)}{\partial\eta^2}+\tilde{F}(\eta;p)\dfrac{\partial^3\tilde{G}(\eta;p)}{\partial\eta^3}+\\+\tilde{G}(\eta;p)\dfrac{\partial^3\tilde{G}(\eta;p)}{\partial\eta^3}\end{array}\right)+\\&+\mathrm{We}\left(\begin{array}{l}16\,\dfrac{\partial^2\tilde{G}(\eta;p)}{\partial\eta^2}\dfrac{\partial^3\tilde{G}(\eta;p)}{\partial\eta^3}-3\,\dfrac{\partial\tilde{F}(\eta;p)}{\partial\eta}\dfrac{\partial^4\tilde{G}(\eta;p)}{\partial\eta^4}+\dfrac{\partial\tilde{G}(\eta;p)}{\partial\eta}\dfrac{\partial^4\tilde{G}(\eta;p)}{\partial\eta^4}-\tilde{F}(\eta;p)\dfrac{\partial^5\tilde{G}(\eta;p)}{\partial\eta^5}+\\-\tilde{G}(\eta;p)\dfrac{\partial^5\tilde{G}(\eta;p)}{\partial\eta^5}-\dfrac{\partial^2\tilde{G}(\eta;p)}{\partial\eta^2}\dfrac{\partial^3\tilde{F}(\eta;p)}{\partial\eta^3}-3\dfrac{\partial^2\tilde{F}(\eta;p)}{\partial\eta^2}\dfrac{\partial^3\tilde{G}(\eta;p)}{\partial\eta^3}+\\+\lambda\left(8\,\dfrac{\partial^2\tilde{G}(\eta;p)}{\partial\eta^2}\dfrac{\partial^3\tilde{G}(\eta;p)}{\partial\eta^3}-2\dfrac{\partial\tilde{F}(\eta;p)}{\partial\eta}\dfrac{\partial^4\tilde{G}(\eta;p)}{\partial\eta^4}-\dfrac{\partial^2\tilde{G}(\eta;p)}{\partial\eta^2}\dfrac{\partial^3\tilde{F}(\eta;p)}{\partial\eta^3}-3\dfrac{\partial^2\tilde{F}(\eta;p)}{\partial\eta^2}\dfrac{\partial^3\tilde{G}(\eta;p)}{\partial\eta^3}\right)\end{array}\right),\end{aligned} \tag{3.7}$$

in which $p \in [0, 1]$ is the embedding parameter and $\hbar_f, \hbar_g$ are non- zero auxiliary parameters. By Taylor's theorem,

$$\tilde{F}(\eta\,;p) = f_0(\eta) + \sum_{m=1}^{\infty} f_m(\eta)\,p^m, \qquad \tilde{G}(\eta\,;p) = g_0(\eta) + \sum_{m=1}^{\infty} g_m(\eta)p^m. \tag{3.8}$$

The general HAM equations for *mth* order can be given by

$$\mathrm{L}\Big[\big(f_m(\eta) - \chi_m f_{m-1}(\eta)\big), \big(g_m(\eta) - \chi_m g_{m-1}(\eta)\big)\Big] = \big(\hbar_f\ \breve{R}_{f,m}(\eta), \hbar_g\ \breve{R}_{g,m}(\eta)\big), \tag{3.9}$$

with the following boundary conditions

$$f'_m(\eta) = g'_m(\eta) = f_m(\eta) + g_m(\eta) = 0 \qquad \text{At} \qquad \eta = 0 \qquad \text{and} \qquad \eta = 1, \tag{3.10}$$

and

$$\chi_m = \begin{cases} 0, & m \le 1 \\ 1, & m \ge 2 \end{cases} \tag{3.11}$$

$$\breve{R}_{f,m}(\eta) = f''''_{m-1}(\eta) + \mathrm{Re}\sum_{i=0}^{m\text{-}1}\big(g'_i(\eta) f''_{m\text{-}1\text{-}i}(\eta) - f'_i(\eta) f''_{m\text{-}1\text{-}i}(\eta) + f_i(\eta) f'''_{m\text{-}1\text{-}i}(\eta) + g_i(\eta) f'''_{m\text{-}1\text{-}i}(\eta)\big) + \tag{3.12}$$
$$+\mathrm{We}\sum_{i=0}^{m-1}\left(\begin{array}{l} 16 f''_i(\eta) f'''_{m-1-i}(\eta) - 3g''_i(\eta) f'''_{m-1-i}(\eta) - f''_i(\eta) g'''_{m-1-i}(\eta) + f''_i(\eta) f''''_{m-1-i}(\eta) - 3g'_i(\eta) f''''_{m-1-i}(\eta) + \\ -f_i(\eta) f'''''_{m-1-i}(\eta) - g_i(\eta) f'''''_{m-1-i}(\eta) + \lambda\left(\begin{array}{l} 8 f''_i(\eta) f'''_{m-1-i}(\eta) - 3g''_i(\eta) f'''_{m-1-i}(\eta) + \\ -f''_i(\eta) g'''_{m-1-i}(\eta) - 2g'_i(\eta) f''''_{m-1-i}(\eta) \end{array}\right) \end{array}\right).$$

$$\breve{R}_{g,m}(\eta) = g''''_{m-1}(\eta) + \mathrm{Re}\sum_{i=0}^{m-1}\big(f'_i(\eta) g''_{m\text{-}1\text{-}i}(\eta) - g'_i(\eta) g''_{m\text{-}1\text{-}i}(\eta) + f_i(\eta) g'''_{m\text{-}1\text{-}i}(\eta) + g_i(\eta) g'''_{m\text{-}1\text{-}i}(\eta)\big) +$$
$$+\mathrm{We}\sum_{i=0}^{m-1}\left(\begin{array}{l} 16 g''_i(\eta) g'''_{m-1-i}(\eta) - 3f'_i(\eta) g''''_{m-1-i}(\eta) + g'_i(\eta) g''''_{m-1-i}(\eta) - f'_i(\eta) g'''''_{m-1-i}(\eta) - g_i(\eta) g'''''_{m-1-i}(\eta) + \\ -g''_i(\eta) f'''_{m-1-i}(\eta) - 3f''_i(\eta) g'''_{m-1-i}(\eta) + \lambda\left(\begin{array}{l} 8g''_i(\eta) g'''_{m-1-i}(\eta) - 2f'_i(\eta) g''''_{m-1-i}(\eta) + \\ -g''_i(\eta) f'''_{m-1-i}(\eta) - 3f''_i(\eta) g'''_{m-1-i}(\eta) \end{array}\right) \end{array}\right). \tag{3.13}$$

Linear Eqs (3.6)-(3.7) with the boundary conditions (3.8) are solved by the homotopy analysis method (HAM).

4. Results and discussion

4.1. Convergence of HAM solution

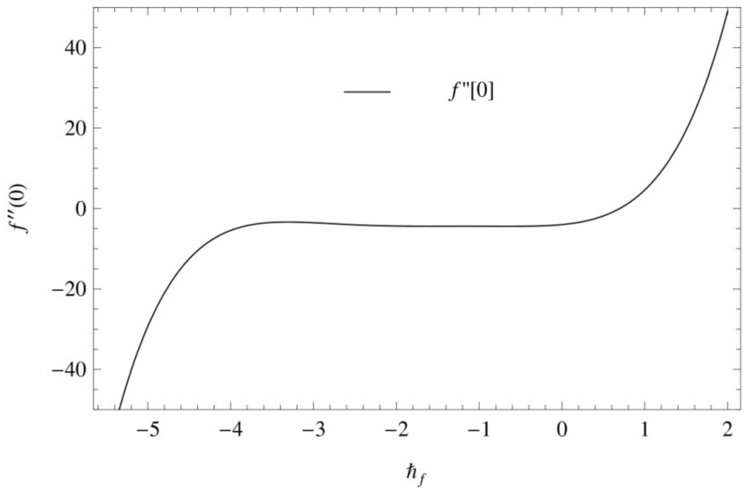

Fig.2. $\hbar_f$ Curve for $f''(0)$ at 7th order approximation.

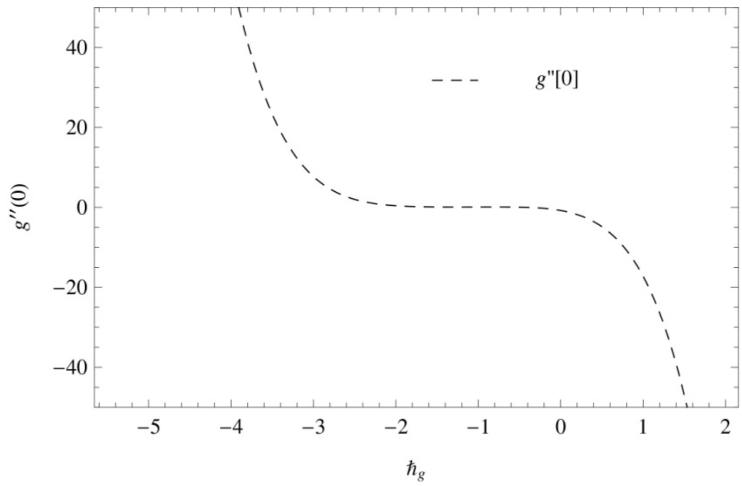

Fig.3. $\hbar_g$ Curve for $g''(0)$ at 7th order approximation.

The auxiliary parameters involved in the definite analytic expressions in Eq.(3.8) are $\hbar_f$ and $\hbar_g$. The convergence region and rate of approximations can be derived for solutions by these parameters. Graphs of $f''(0)$ and $g''(0)$ have been plotted at 7th order of approximations for a considerable range of values of these parameters. Figure 2 shows the admissible values for $\hbar_f$ is $-3.8 \le \hbar_f \le 0.2$ and for $\hbar_g$ is $-2.6 \le \hbar_g \le -0.2$.

4.2. Discussion on graphs

This subsection focuses on the influence of emerging parameters on the velocity profile $f'(\eta)$. Figure 4 demonstrates the effect of the suction parameter w_0 on the velocity component $f'(\eta)$ graph at keeping the upper wall to be nonporous as $(w_1 = 0)$. It is shown that the velocity starts to rise. It is observed that large values of the suction parameter w_0 depreciate the reverse flow, by virtue of this the skin friction at the stretching wall increases. In Fig.5 it can be noticed that the velocity increases at very small values of w_0 in the presence of an upper wall injection. It can also be seen that the velocity increases rapidly by increasing the value of w_0 and it disappears the reverse flow. Figure 6 illustrates mass transfer phenomenon from the upper plate to the lower plate. In a channel flow both walls are taken as porous sheets and it has been assumed that both walls are subjected to mass transfer. Further, from Fig.7 it can be seen that both walls of the channel are subjected to uniform injection. In this case the velocity component increases to a certain value of η and then it will decrease. Figure 8 shows that when both walls are subjected to uniform suction, a reverse flow of velocity develops significantly. From Figs 7 and 8, it can be concluded that velocity overshoot and reverse flow can be controlled by mass transfer. Figure 9 shows the shear rate at the stretching wall against w_1 for various values of w_0. At a fixed value of w_0 it gives appropriate values of w_1 in order to reduce the viscous drag. Figure 10 shows the influence of the parameter λ on the velocity component $f'(\eta)$ which illustrates that an increment in the values of λ increases the velocity in one direction.

Figure 11 shows the same behaviour as in Fig.10 by changing the values of We. Figure 12 shows that the velocity component $f'(\eta)$ increases with increasing values of Re. Numerical results are shown in Tabs 1-6. The tables show the calculation of our solutions at different orders of approximation.

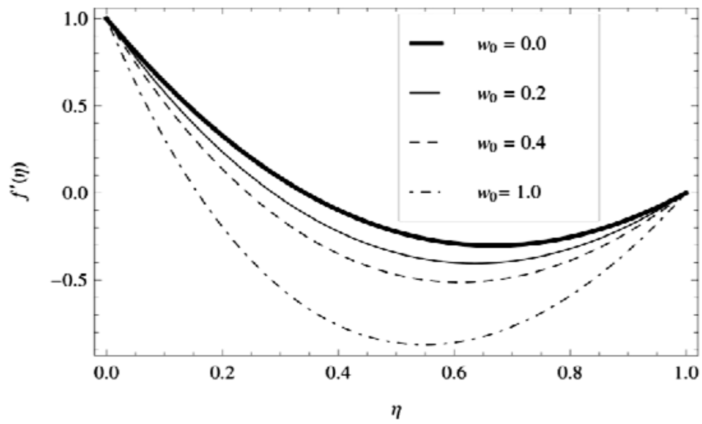

Fig.4. The effect of the parameter w_0 on $f'(\eta)$ for $w_1 = 0$, We $= 0.01, \hbar = -0.8$, Re $= 2.0$, $\lambda = 0.01$ and $\beta = 0.5$.

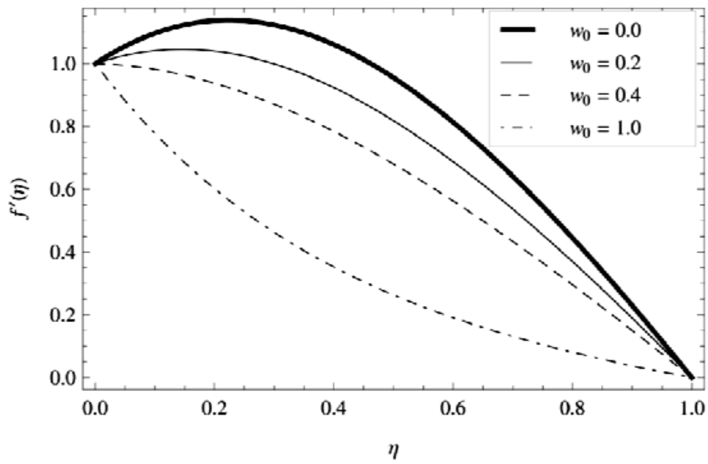

Fig.5. The effect of the parameter w_0 on $f'(\eta)$ for $w_1 = 1.5$, We $= 0.01, \hbar = -0.8$, Re $= 2.0$, $\lambda = 0.01$ and $\beta = 0.5$.

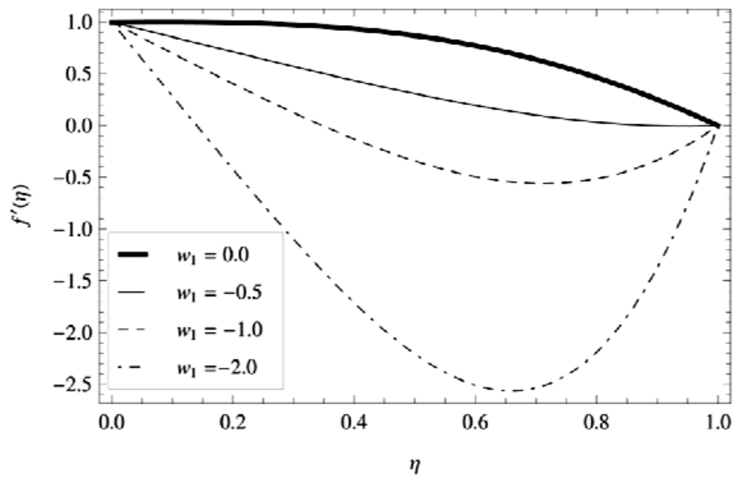

Fig.6. Velocity $f'(\eta)$ by reversing the direction of mass transfer at $\hbar = -0.8$, $\lambda = 0.01$, $\mathrm{We} = 0.02$, $\mathrm{Re} = 2.0$, $w_0 = -2.0$ and $\beta = 0.5$.

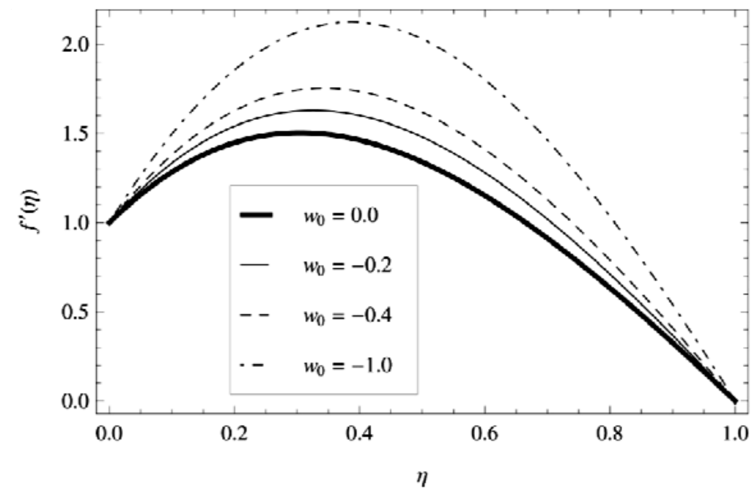

Fig.7. The effect of injection on $f'(\eta)$ at $\hbar = -0.8$, $\lambda = 0.01$, $\mathrm{We} = 0.01$, $\mathrm{Re} = 2.0$, $w_1 = 2.0$ and $\beta = 0.5$.

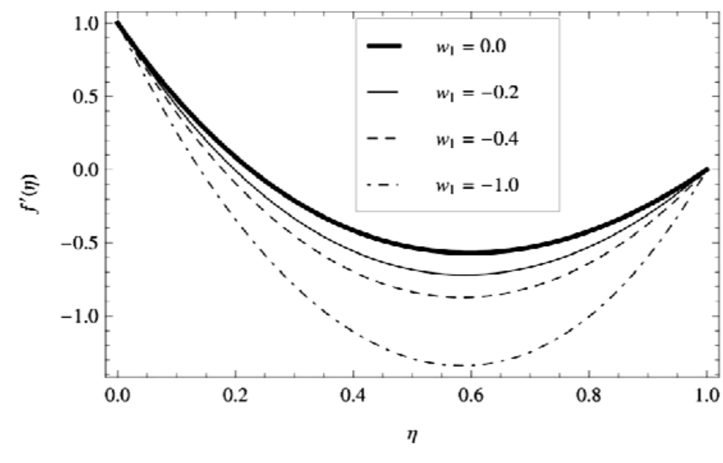

Fig.8. The effect of suction on $f'(\eta)$ at $\hbar = -0.8$, $\lambda = 0.01$, $\mathrm{We} = 0.01$, $\mathrm{Re} = 2.0$, $w_0 = 0.5$ and $\beta = 0.5$.

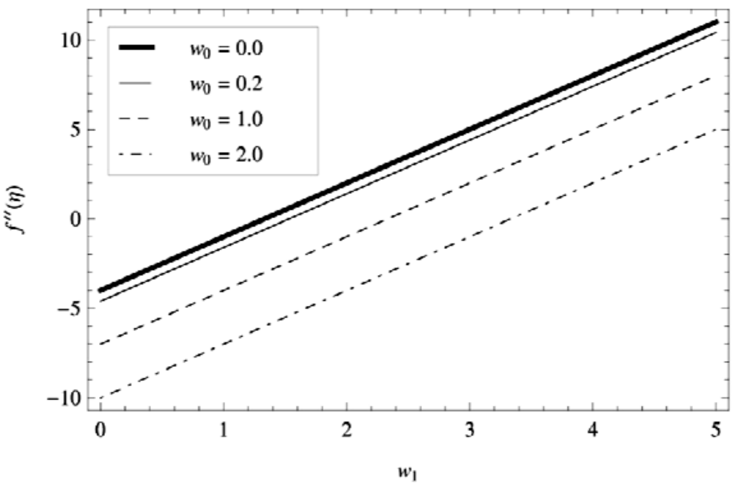

Fig.9. Velocity gradient at the plate vs. w_1 at $\hbar = -0.8$, $\lambda = 0.01$, $\mathrm{We} = 0.1$, $\mathrm{Re} = 2.0$, $\eta = 0$ and $\beta = 0.5$.

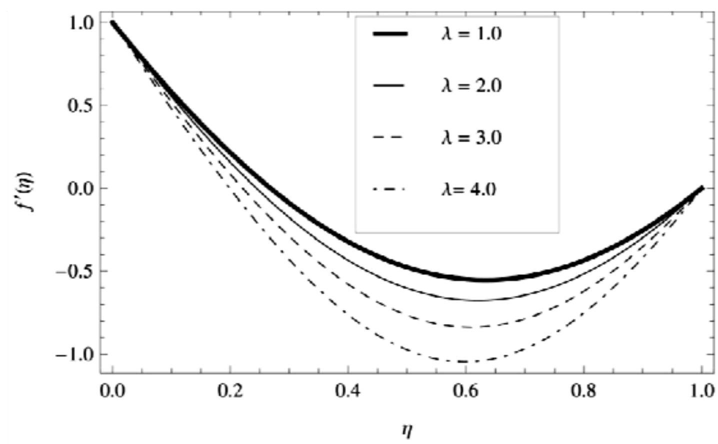

Fig.10. The influence of the parameter λ on $f'(\eta)$ at $\hbar = -0.8$, $\mathrm{We} = 0.02$, $\mathrm{Re} = 0.03$, $w_1 = w_0 = 0.05$ and $\beta = 0.5$.

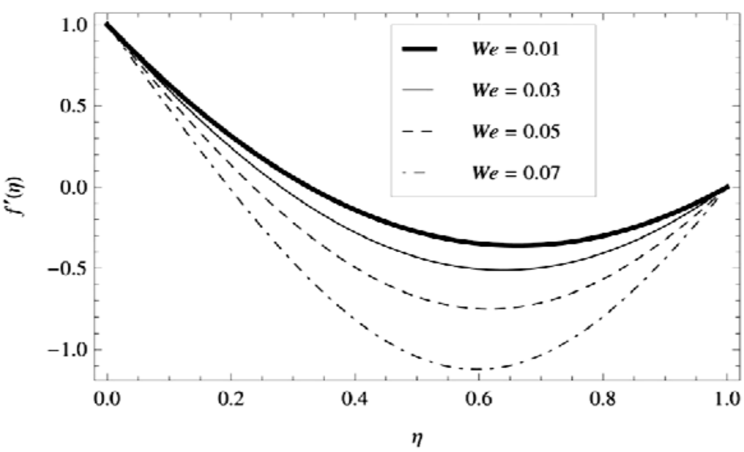

Fig.11. The influence of the parameter We on $f'(\eta)$ at $\hbar = -0.8$, $\lambda = 0.01$, $\mathrm{Re} = 0.01$, $w_1 = 0.05$, $w_0 = 0.01$ and $\beta = 0.5$.

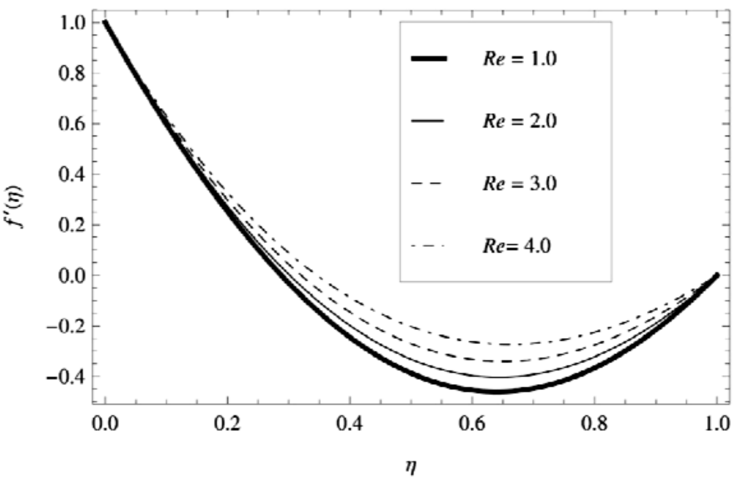

Fig.12. The influence of the parameter Re on $f'(\eta)$ at $\hbar = -0.8$, $\lambda = 0.6$, $\mathrm{We} = 0.02$, $w_1 = w_0 = 0.05$ and $\beta = 0.5$.

5. Numerical values at different orders of approximation

Table 1. The variation of $-f''(0)$ for various We and λ at $\hbar = -0.8$, $\beta = w_0 = w_1 = 0.5$ and $\mathrm{Re} = 2.0$ at 2nd order of approximation.

We / λ	0	0.1	0.2	0.3	0.4
0	4.1223	5.42253	8.43438	13.1579	19.5929
0.1	4.1223	5.54464	8.86189	14.0741	21.1812
0.2	4.1223	5.67161	9.30888	15.0341	22.8473
0.3	4.1223	5.80345	9.77534	16.038	24.5914
0.4	4.1223	5.94016	10.2613	17.0857	26.4133

Table 2. The variation of $-g''(0)$ for various We and λ at $\hbar = -0.8$, $\beta = w_0 = w_1 = 0.5$ and $\mathrm{Re} = 2.0$ at 2nd order of approximation.

We / λ	0	0.1	0.2	0.3	0.4
0	2.93998	0.239006	-4.22427	-10.4498	-18.4377
0.1	2.93998	0.042245	-4.85395	-11.7486	-20.6418
0.2	2.93998	-0.161436	-5.51132	-13.1097	-22.9565
0.3	2.93998	-0.372036	-6.19636	-14.533	-25.382
0.4	2.93998	-0.589556	-6.90908	-16.0186	-27.9181

Table 3. The variation of $-f''(0)$ for various We and λ at $\hbar = -0.8$, $\beta = w_0 = w_1 = 0.5$ and $\mathrm{Re} = 2.0$ at 4th order of approximation.

We / λ	0	0.1	0.2	0.3	0.4
0	4.16205	6.48427	18.1202	50.5349	119.943
0.1	4.16205	6.80138	20.3068	58.1717	139.409
0.2	4.16205	7.14589	22.7157	66.6237	160.994
0.3	4.16205	7.51904	25.3584	75.9361	184.82
0.4	4.16205	7.9221	28.2468	86.1543	211.007

Table 4. The variation of $-g''(0)$ for various We and λ at $\hbar = -0.8$, $\beta = w_0 = w_1 = 0.5$ and $\mathrm{Re} = 2.0$ at 4th order of approximation.

We / λ	0	0.1	0.2	0.3	0.4
0	2.96693	-1.58619	-23.8697	-92.2035	-247.883
0.1	2.96693	-2.16961	-28.7061	-111.432	-301.427
0.2	2.96693	-2.81342	-34.1854	-133.438	-363.04
0.3	2.96693	-3.52186	-40.3626	-158.478	-433.493
0.4	2.96693	-4.29934	-47.2945	-186.819	-513.593

Table 5. The variation of $-f''(0)$ for various We and λ at $\hbar = -0.8$, $\beta = w_0 = w_1 = 0.5$ and $\mathrm{Re} = 2.0$ at 5th order of approximation.

We / λ	0	0.1	0.2	0.3	0.4
0	4.16364	6.69439	18.3573	35.1417	18.3082
0.1	4.16364	7.04537	19.6426	30.9893	-22.2192
0.2	4.16364	7.42132	20.6812	23.1378	-18.6256
0.3	4.16364	7.82107	21.3615	10.5847	-164.44
0.4	4.16364	8.24298	21.5544	-7.81368	-275.798

Table 6. The variation of $-g''(0)$ for various We and λ at $\hbar = -0.8$, $\beta = w_0 = w_1 = 0.5$ and $\mathrm{Re} = 2.0$ at 5th order of approximation.

We / λ	0	0.1	0.2	0.3	0.4
0	4.1223	5.42253	8.43438	13.1579	19.5929
0.1	4.1223	5.54464	8.86189	14.0741	21.1812
0.2	4.1223	5.67161	9.30888	15.0341	22.8473
0.3	4.1223	5.80345	9.77534	16.038	24.5914
0.4	4.1223	5.94016	10.2613	17.0857	26.4133

Table 7. A comparison of present solution and [20] for velocity functions $f''(0)$ and $g''(0)$.

Re	0.5	1.0	1.5	2.0	2.5
$f''(0)$ Present Solution	4.01733	4.05095	4.10001	4.16364	4.24093
[20]	4.01649	4.04796	4.094	4.15418	4.22808
$g''(0)$ Present Solution	2.24558	2.4891	2.72998	2.96796	3.20305
[20]	2.24381	2.48597	2.72592	2.96311	3.19699

6. Concluding remarks

The present article describes the three dimensional second grade fluid flow in a channel of lower stretching wall. Injection is carried into one plate and suction from another plate. Mass transfer is very helpful to control such types of flow. The basic equations governing the flow have been reduced to a set of nonlinear differential equations using similarity transformations. These nonlinear differential equations have been solved by means of HAM. We inspect quantitatively and qualitatively the influence of different parameters on the flow in a channel.

The following conclusions can be obtained from the graphical results:

- Convergence regions for f and g have been investigated at 7th order of approximations for acceptable values of auxiliary parameters $\hbar_f$ and $\hbar_g$.
- It is noticed that the velocity initially increases in the absence of the upper wall injection parameter ($w_1 = 0$) but after reaching some point, the velocity graph is inversely related to the suction parameter w_0 and it starts to decline after getting increasing values of the suction parameter w_0 and shows reverse flow.
- The variation of the suction parameter w_0 increases the velocity component $f'(\eta)$ in the presence of upper wall injection.
- It is observed that transferring of mass from the upper plate to the lower plate is considered in order to decrease the viscous drag on stretching sheet.
- It has been shown that when both walls are subjected to injection, then velocity grows up to a certain value of η and then it decreases.
- Further, it has been demonstrated that a reverse flow has been seen when both walls are subjected to uniform suction.
- In favor to reduce the viscous drag then graph of shear stress against w_1 has been made.
- The velocity component $f'(\eta)$ increases toward one direction with increasing values of λ and We.
- It can be seen that the velocity component $f'(\eta)$ increases with increasing values of Re.
- It can be seen from the tables that convergence of HAM solution can be obtained by taking higher orders of approximation.

Nomenclature

A_1, A_2 – kinematical tensors
a, b – velocity gradients
f, g – dimensionless stream function
h – width of the channel
$\boldsymbol{I}$ – unit vector
p – pressure
p_0 – pressure at the origin
Re – local Reynolds number
T – extra stress tensor
u – x-component of fluid velocity
v – y-component of fluid velocity
We – Weissenberg number
w – z-component of fluid velocity
w_0^*, w_1^* – suction/ injection velocities at the lower and upper walls
α_1, α_2 – normal stress moduli
β – ratio of velocity gradients
η – similarity variable
λ – ratio of normal stress moduli
μ – coefficient of shear viscosity
ν – kinematic viscosity
ρ – density of the fluid
τ_{xz} – skin friction coefficient in the x – direction
τ_{yz} – skin friction coefficient in the y – direction
∇ – gradient operator

References

[1] Dunn J.E. and Fosdick R.L. (1974): *Thermodynamics, stability and boundedness of fluids of complexity 2 and fluids of second grade*. – Arch. Ration. Mech. Anal., vol.56, pp.191-252.

[2] Dunn J.E. and Rajagopal K.R. (1995): *Fluids of differential type-critical review and thermodynamic analysis*. – Int. J. Eng. Sci., vol.33, pp.689-729.

[3] Ali S.A., Ara A. and Khan N.A. (2007): *Martin's method applied to steady plane flow of a second grade fluid.* – Int. J. Appl. Math. Mech., vol.3, pp.71-81.

[4] Mahmood A., Khan N.A., Fetecau C., Jamil M. and Rubbab Q. (2009): *Exact analytic solutions for the flow of second grade fluid between two longitudinally oscillating cylinder*. – J. Prime Research in Math., vol.5, pp.192-204.

[5] Hayat T., Khan M., Ayub M. and Siddiqui A.M. (2005): *The unsteady Couette flow of second grade fluid in a layer of porous medium*. – Arch. Mech., vol.57, pp.405-416.

[6] Abdallah I.A. (2009): *Analytical solution of heat and mass transfer over a permeable stretching plate affected by a chemical reaction, internal heating, Dufour-Souret effect and Hall effect*. – Int. J. Therm. Sci., vol.2, pp.183-197.

[7] Ariel P.D. (2002): *On exact solutions of flow problems of a second grade fluid through two parallel porous walls*. – Int. J. Eng. Sci., vol.40, pp.913-941.

[8] Chen C.I., Chen C.K. and Yang Y.T. (2003): *Unsteady unidirectional flow of a second grade fluid between the parallel plates with different given volume flow rate conditions*. – Appl. Math. Comput., vol.137, pp.437-450.

[9] Aksoy Y., Pakdemirli M. and Khalique C.M. (2007): *Boundary layer equations and stretching sheet solutions for the modified second grade fluid.* – Int. J. Eng. Sci., vol.45, pp.829-841.

[10] Hayat T. and Sajid M. (2007): *Analytical solution for axisymmetric flow and heat transfer of a second grade fluid past a stretching sheet*. – Int. J. Heat Mass Transfer, vol.50, pp.75-84.

[11] Galdi G.P. and Sequeira A. (1994): *Further existence results for classical solutions of the equations of second-grade fluid*. – Arch. Rat. Mech. Anal., vol.128, pp.297-312.

[12] Cortell R. (2007): *MHD flow and mass transfer of an electrically conducting fluid of second grade in a porous medium over a stretching sheet with chemically reactive species*. – Chem. Eng. Process., vol.46, pp.721-728.

[13] Ellahi R. (2013): *The effects of MHD and temperature dependent viscosity on the flow of non-Newtonian nanofluid in a pipe: Analytical solutions*. – Appl. Math. Model., vol.37, pp.1451-1467.

[14] Hayat T., Qasim M. and Abbas Z. (2010): *Homotopy solution for unsteady three-dimensional MHD flow and mass transfer in a porous space.* – Commun. Nonlinear Sci. Numer. Simul., vol.15, pp.2375-2387.

[15] Hayat T., Mustafa M. and Mesloub S. (2010): *Mixed convection boundary layer flow over a stretching surface filled with a Maxwell fluid in presence of Soret and Dufour effects*. – Z. Naturforsch., vol.65, pp.401-410.

[16] Abel M.S., Mahesha N. and Malipatil S.B. (2011): *Heat transfer due to MHD slip flow of a second-grade liquid over a stretching sheet through a porous medium with non uniform heat source/sink.* – Chem. Eng. Commun., vol.198, pp.191-213.

[17] Zeeshan A. and Ellahi R. (2013): *Series solutions for nonlinear partial differential equations with slip boundary conditions for non-Newtonian MHD fluid in porous space*. – J. Appl. Math. Inf. Sci., vol.7, pp.257-265.

[18] Ellahi R., Wang X. and Hameed M. (2014): *Effects of heat transfer and nonlinear slip on the steady flow of Couette fluid by means of Chebyshev spectral method*. – Z. Naturforsch. A, vol.69, pp.1-8.

[19] Sheikholeslami M., Ellahi R., Ashorynejad H.R., Domairry G. and Hayat T. (2014): *Effects of heat transfer in flow of nanofluids over a permeable stretching wall in a porous medium*. – Comput. Theor. Nanosci., vol.11, pp.486-496.

[20] Mehmood A. and Ali A. (2011): *Across mass transfer phenomenon in a channel of lower stretching wall.* – Chem. Eng. Commun., vol.198, pp.678-691.

[21] Tamayol A., Hooman K. and Bahrami M. (2010): *Thermal analysis of flow in a porous medium over a permeable stretching wall*. – Transp. Porous Med., vol.85, pp.661-676.

[22] Raftari B. and Vajravelu K. (2012): *Homotopy analysis method for MHD viscoelastic fluid flow and heat transfer in a channel with a stretching wall*. – Commun. Nonlinear Sci. Numer. Simulat., vol.17, pp.4149-4162.

[23] Mehmood A. and Ali A. (2010): *Heat transfer analysis of three-dimensional flow in a channel of lower stretching wall*. – J. Taiwan Inst. Chem. Eng., vol.41, pp.29-34.

[24] Munawar S., Mehmood A. and Ali A. (2012): *Three-dimensional squeezing flow in a rotating channel of lower stretching porous wall*. – Comp. Math. Appl., vol.64, pp.1575-1586.

[25] Alhuthali M.S., Shehzad S.A., Malaikah H. and Hayat T. (2014): *Three dimensional flow of viscoelastic fluid by an exponentially stretching surface with mass transfer*. – J. Pet. Sci. Eng., vol.119, pp.221-226.

[26] Nadeem S., Rizwan Ul Haq, Akbar N.S. and Khan Z.H. (2013): *MHD three-dimensional Casson fluid flow past a porous linearly stretching sheet*. – Alexandria Engineering Journal, vol.52, pp.577-582.

[27] Qasim M. (2013): *Heat and mass transfer in a Jeffrey fluid over a stretching sheet with heat source/sink*. – Alexandria Engineering Journal, vol.52, pp.571-575.

[28] Abel M.S., Nandeppanavar M.M. and Malipatil S.B. (2010): *Heat transfer in a second grade fluid through a porous medium from a permeable stretching sheet with non-uniform heat source/sink*. – Int. J. Heat Mass Transfer, vol.53, pp.1788-1795.

[29] Hayat T., Awais M. and Obaidat S. (2012): *Three-dimensional flow of a Jeffery fluid over a linearly stretching sheet*. – Commun. Nonlinear Sci. Numer. Simulat., vol.17, pp.699-707.

[30] Liao S.J. (1992): *The proposed homotopy analysis technique for the solution of nonlinear problems*. – PhD Thesis, Shanghai Jiao Tong University.

[31] Khan N.A., Aziz S. and Nadeem. A. Khan (2014): *MHD flow of Powell-Eyring fluid over a rotating disk*. – J. Taiwan Inst. Chem. E., vol.45, pp.2859-2867.

[32] Khan N.A. and Riaz F. (2014): *Off-centred stagnation point flow of a couple stress fluid towards a rotating disk.* – The Scientific World Journal, Article ID 163586.

Received: March 10, 2015

Revised: May 10, 2016